Articles in PresS. Am J Physiol Endocrinol Metab (July 27, 2010). doi:10.1152/ajpendo.00323.2010

Intense Electro-Acupuncture Normalizes Insulin Sensitivity, Increases Muscle GLUT4 Content, and Improves Lipid Profile in a Rat Model of Polycystic Ovary Syndrome

Julia Johansson [1], Yi Feng [2], Ruijin Shao [1], Malin Lönn [3], Håkan Billig [1], Elisabet Stener-Victorin * [1, 4]

[1] *Institute of Neuroscience and Physiology, Department of Physiology, Sahlgrenska Academy, University of Gothenburg, Sweden*

[2] *Department of Neurobiology and Integrative Medicine, Shanghai Medical College of Fudan University, Shanghai, China*

[3] *Institute of Biomedicine, Department of Clinical Chemistry and Transfusion Medicine, Sahlgrenska Academy, University of Gothenburg, 405 30 Gothenburg, Sweden*

[4] *Department of Obstetrics and Gynecology, First Affiliated Hospital, Heilongjiang University of Chinese Medicine, Harbin 150040, China*

Running title: Acupuncture, GLUT4 muscle content and lipid profile

*** Corresponding author and reprint requests**
Elisabet Stener-Victorin
Institute of Neuroscience and Physiology
Department of Physiology
Sahlgrenska Academy
Göteborg University, Box 434
SE-405 30 Göteborg, Sweden
Tel: +46(0)31 7863557
Fax: +46(0)31 7863512
E-mail: elisabet.stener-victorin@neuro.gu.se

ABSTRACT

Polycystic ovary syndrome (PCOS) is associated with hyperandrogenism and insulin resistance, possibly reflecting defects in skeletal muscle and adipocyte insulin signaling. Low-frequency (2 Hz) electro-acupuncture (EA) increases insulin sensitivity in female rats with dihydrotestosterone (DHT)-induced PCOS, but the mechanism is unclear. We hypothesized that low-frequency EA regulates mediators involved in skeletal muscle glucose uptake and metabolism and alters the lipid profile in rats with DHT-induced PCOS. To test this hypothesis, we implanted in prepubescent female rats 90-d continuous-release pellets containing DHT (PCOS). At 70 d of age, the rats were randomly subdivided into two groups: one received low-frequency EA (evoking muscle twitches) for 20–25 min, five times/wk for 4–5 wks; the other did not. Controls were implanted with pellets containing vehicle only. All three groups were otherwise handled similarly. Lipid profile was measured in fasting blood samples. Insulin sensitivity was determined by euglycemic-hyperinsulinemic clamp, soleus muscle protein expression of glucose transporter 4 (GLUT4) and phosphorylated and nonphosphorylated Akt and Akt substrate of 160 kDa were determined by Western blot analysis and GLUT4 location by immunofluorescence staining. PCOS EA rats had normalized insulin sensitivity, lower levels of total, high density lipoprotein, and low density lipoprotein cholesterol, and increased expression of GLUT4 in different compartments of skeletal muscle compared with PCOS rats. Total weight and body composition did not differ in the groups. Thus, in rats with DHT-induced PCOS, low-frequency EA has systemic and local effects involving intracellular-signaling pathways in muscle that may, at least in part, account for the marked improved insulin sensitivity.

Keywords

Acupuncture, GLUT4, insulin resistance, lipids, muscle contraction, skeletal muscle

INTRODUCTION

Hyperandrogenemia is the most prominent endocrine phenotype in women with polycystic ovary syndrome (PCOS) (56), in addition to ovulatory dysfunction and polycystic ovary morphology (3). The main metabolic phenotype is hyperinsulinemia and insulin resistance, which are independent of body weight (19, 40). Other metabolic abnormalities associated with insulin resistance are obesity, dyslipidemia, and increased risk for type 2 diabetes.

The mechanisms for the association between endocrine and metabolic abnormalities in PCOS are unclear (13, 18). PCOS is characterized by clinical and/or biochemical hyperandrogenism. In female rats and humans, exogenous exposure to testosterone or dihydrotestosterone (DHT) leads to insulin resistance and obesity (4, 14, 17, 22, 50, 58). The insulin resistance in women with PCOS is associated with a dyslipidemia characterized by low levels of high density lipoprotein (HDL) cholesterol and high levels of low density lipoprotein (LDL) and triglycerides (TG) (49).

Women with PCOS display both insulin resistance and reduced insulin responsiveness (11). The insulin resistance has been attributed to defects in insulin signaling in adipocytes and skeletal muscle (11, 12, 20, 21). In female rats, testosterone exposure results not only in obesity and insulin resistance but also in changes in muscle morphology, including a reduction in type 1 fibers, an increase in type 2 fibers, and decreased capillary density (30, 31). After testosterone exposure, insulin-mediated glucose uptake is reduced, most likely because of impairments in glycogen synthase expression and plasma membrane translocation of glucose transporter 4 (GLUT4) in skeletal muscle (58). Indeed, women with PCOS, have reduced GLUT4 content in both whole-cell lysates and membrane preparations of adipose tissue (60, 62). Further, GLUT4 translocation stimulated by insulin or contractions in skeletal muscle is dependent on phosphorylation of the Akt substrate of 160 kDa (AS160) (38, 39, 61). Recent findings suggest

that insulin resistance in women with PCOS reflects impaired phosphorylation of Akt and AS160 in skeletal muscle (11, 32). Thus, hyperandrogenism and PCOS are associated with molecular alterations in skeletal muscle and adipose tissue that may explain, at least in part, the decreased insulin sensitivity.

Treatment of PCOS is symptom-oriented however unsatisfactory in a wider perspective. Physical exercise and diet are the first-line options for treating and preventing metabolic dysfunction, both generally and in women with PCOS (55). In a rat model of DHT-induced PCOS that exhibits both ovarian and metabolic characteristics of the syndrome (50), low-frequency (2 Hz) electro-acupuncture (EA) *and* physical exercise—both of which induce muscle contraction—increase insulin sensitivity and modulate gene expression in adipose tissue. Unlike exercise, EA does not reduce adipose tissue mass (51, 52). Consistent with these results, in Goto-Kakizaki rats, a genetic model of type 2 diabetes, EA improves hyperglycemia and restores impaired glucose tolerance by enhancing insulin sensitivity (33). Further, in mice with diet-induced hypercholesterolemia, EA had a cholestrol-lowering effect similar to that of simvastatin (35, 41).

The mechanism for the beneficial effects of 4–5 weeks of low-frequency EA given 3 d per week is unknown (51, 52). Most likely, it involves a direct influence on skeletal muscle signaling mechanisms and secondary actions in adipose tissue. Muscle contraction during low-frequency EA may stimulate glucose uptake via an insulin-independent pathway and may be mediated, at least in part, by signaling pathways in skeletal muscle similar to those activated by chronic exercise (16, 25). The signaling mechanisms in skeletal muscle after muscle contraction have been extensively studied (59). Few such studies have been conducted on low-frequency EA. In male rats acutely exposed to prednisolone to induce an insulin-resistant state, low-frequency EA

for 60 min during anesthesia restored protein expression of insulin receptor substrate 1 and GLUT4 in skeletal muscle (45). The mechanism by which low-frequency EA improves insulin sensitivity in rats with DHT-induced PCOS remains to be elucidated. Further, it is not known whether low-frequency EA can restore normal insulin sensitivity, as exercise does, when EA is given more frequently in rats with DHT-induced PCOS.

In this study, we tested the hypothesis that low-frequency EA, given 5 d per week for 4–5 weeks at an intensity high enough to evoke muscle twitches would normalize insulin sensitivity by restoring signaling mechanisms in skeletal muscle and improve the lipid profile of DHT-induced PCOS rats. We measured whole-body insulin sensitivity by euglycemic-hyperinsulinemic clamp test, body composition by dual emission x-ray absorptiometry (DEXA), the lipid profile by ELISA, and skeletal muscle protein expression and activation of GLUT4, Akt, and AS160 by western blot and GLUT4 location by immunofluorescence staining.

MATERIALS AND METHODS

Animals

Four Wistar dams, each with eight or nine female pups, were purchased from Charles River (Sulzfeld, Germany). Pups were raised with a lactating dam until 21 d of age and housed four to five per cage under controlled conditions (21–22°C, 55–65% humidity, 12-h light/12-h dark cycle). Rats were fed commercial chow (Harlan Teklad Global Diet, 16% protein rodent diet (2016, Harlan Winkelmann, Harlan, Germany) and tap water *ad libitum*. Animals were cared for in accordance with the principles of the Guide to the Care and Use of Experimental Animals (www.sjv.se). The study was approved by the Animal Ethics Committee of the University of Gothenburg.

Study procedure

At 21 d of age, rats were randomly divided into three experimental groups (control, PCOS, and PCOS EA; n=12 per group) and implanted subcutaneously with 90-day continuous-release pellets (Innovative Research of America, Sarasota, FL) containing 7.5 mg of DHT (daily dose, 83 μg) or 7.5 mg of vehicle. In our previous study, this dose of DHT resulted in PCOS characteristics, including metabolic disturbances at adult age (50). All rats were weighed weekly from 21 d of age. A microchip (AVID, Norco, CA) with an identification number was inserted in the neck along with the pellets. EA treatments started at 70 d of age, 7 weeks after the start of DHT exposure. The study was concluded after 12 weeks of DHT exposure, including 4–5 weeks of treatment with low-frequency EA.

Treatment

Low-frequency EA was given to conscious rats daily, Monday to Friday, for 4–5 weeks (20–25 treatments in total). The treatment duration was 15 min in week 1, 20 min in weeks 2 and 3, and 25 min thereafter. Acupuncture needles were inserted in the rectus abdominis and in the solues and gastrocnemius muscles forming the triceps surae muscles bilaterally, in the somatic segments corresponding to innervation of the ovaries (i.e., from spinal levels T10 to L2 and at the sacral level). The needles (HEGU Svenska, Landsbro, Sweden) were inserted to a depth of 0.5–0.8 cm, attached to an electric stimulator (CEFAR ACU II; Cefar-Compex Scandinavia, Malmo, Sweden), and stimulated with at 2 Hz with 0.1-sec, 80-Hz burst pulses (51, 53, 69-71). The intensity varied from 0.8–1.4 mA during stimulation and was adjusted to produce local muscle contractions. Owing to receptor adaptation, the amplitude was adjusted when muscle contractions become invisible. Usually the amplitude was adjusted after 5 min of stimulation, and most rats tolerated higher amplitudes at the end of the each treatment. All rats tolerated the full treatment for 4–5 weeks.

Before handling or needle insertion, all rats were lightly anesthetized with isoflurane (2% in a 1:1 mixture of oxygen and air; Isoba Vet; Schering-Plough, Stockholm, Sweden) for 2–3 min. One investigator inserted all needles. During EA treatment, rats were placed in a fabric harness and suspended above the desk. All rats were conscious during handling and treatment. Rats in the control and PCOS groups were anesthetized, suspended in a harness, and handled in the same way as rats in the PCOS EA group except for needle insertion and electrical stimulation. No treatment was performed 24 h before examinations and blood sampling.

Vaginal smears

The stage of cyclicity was determined by microscopic analysis of the predominant cell type in vaginal smears obtained daily from the onset of EA treatment at 70 days of age to the end of the experiment (54).

Blood sampling and body composition

At 14 weeks of age (4 weeks of treatment, 10 weeks after pellet implantation), tail blood was obtained to assess the lipid profile. Plasma samples were stored at –80°C until analyses. Body composition was also assessed at 14 weeks. Rats were lightly anesthetized by inhalation of isoflurane (Abbott Scandinavia, Solna, Sweden; 2% in 1:1 mixture of oxygen and air) and analyzed with a whole-body DEXA instrument (QDR-1000/W, Hologic, Waltham, MA). Total body fat, lean body mass, and bone mineral content were determined for each rat.

Euglycemic-hyperinsulinemic clamp and sample collection

At 15–16 weeks of age (5 weeks of treatment, 11–12 weeks after pellet implantation), rats were subjected to a euglycemic-hyperinsulinemic clamp (27), during the estrous phase if cycling. PCOS rats without treatment displayed chronic pseudoestrus. Rats were anesthetized with thiobutabarbital sodium (130 mg/kg ip; Inactin; Sigma-Aldrich, St. Louis, MO) and body

166 temperature was maintained at 37˚C with a heating pad throughout the clamp. Catheters were
167 inserted into the left carotid artery for blood sampling and into the right jugular vein for glucose
168 and insulin infusions; to facilitate breathing, a tracheotomy was performed. Insulin (100 U/ml
169 Actrapid; Novo Nordisk, Bagsvaerd, Denmark) together with 0.2 ml of albumin and 10 ml of
170 physiological saline was infused at 24, 16, and 12 mU/min/kg for 1, 2, and 3 min, respectively,
171 followed by 8 mU/min/kg for the rest of the clamp. Blood glucose was analyzed (10 µl) with a
172 B-glucose analyzer (HemoCue, Dronfield, Derbyshire, UK); 20% glucose in saline solution was
173 continuously administered to maintain plasma glucose at a constant euglycemic level (6.0 mM).
174 The glucose infusion rate (GIR) was guided by glucose concentration measurements every 5
175 min. At steady-state (after 50–70 min), mean GIR was normalized to body weight, and blood
176 samples were taken to determine plasma insulin concentrations.

177 After the experiment, the rats were decapitated, and hind limb muscles (soleus,
178 gastrocnemius, and extensor digitorum longus) and fat depots (parametrial, retroperitoneal,
179 inguinal, and mesenteric) were dissected and weighed. Soleus muscle was stabilized in RNAlater
180 (Qiagen, Hilden, Germany) for 12 h and stored at –80˚C until protein analyses.

181 *Biochemical analyses*

182 Plasma concentrations of total cholesterol (ref 981813), HDL (ref 981655) and LDL (ref
183 981656) cholesterol, and TG (ref 981786) were determined enzymatically; HDL was determined
184 after precipitation of apolipoprotein B–containing lipoproteins with magnesium sulfate and
185 dextran sulfate (Thermo Fisher Scientific, Vantaa, Finland). All analyses were performed on a
186 Konelab 20 autoanalyzer (Thermo Fisher Scientific); the interassay coefficients of variation were
187 <3%. All lipid analyses were carried out at an accredited laboratory at the Wallenberg
188 Laboratory, Sahlgrenska University Hospital, Sweden. Basal insulin and human insulin, given

during the clamp, were measured in duplicate with ELISA kits (ref 10-1124-01 and ref 10-1113-01, respectively; Mercodia, Uppsala, Sweden).

Homogenization

Frozen tissue was placed in ice-cold RIPA buffer (150 mM NaCl, 1.0% IGEPAL CA-630, 0.5% sodium deoxycholate, 0.1% SDS, 50 mM Tris, pH 8.0) (Sigma-Aldrich) containing 1x complete protease inhibitor cocktail and phosphatase inhibitor cocktail (PhosSTOP, Roche Diagnostics, Basel, Switzerland) and homogenized twice for 3 min each with a tissueLyser (Qiagen) at 25 Hz. Homogenate samples were rotated on ice for 45 min and centrifuged (16,300 x g) for 20 min at 4°C. Supernatants were collected, and protein concentration was determined with a BCA protein assay kit (Pierce Biotechnology, Rockford, IL) according to the manufacturer's protocol. The rest was stored at –80° C until further analyses.

Immunoblotting

Total protein (~30 or 50 μg) was separated by SDS-PAGE and transferred to nitrocellulose or PVDF. Membranes were rinsed in Tris-buffered saline with 0.1% Tween-20 (TBS-T), blocked in 5% non-fat dry milk in TBS-T for 1 h in room temperature and incubated in primary antibody over night at 4˚C. The following day, blots were washed in TBS-T, incubated in secondary antibody for 1 h in room temperature and washed again in TBS-T. Protein bands were developed with SuperSignal West Dura Extended Duration Substrate (Pierce Biotechnology, Rockford, IL) and photographed with an LAS-1000 camera system (Fujifilm, Tokyo, Japan). The intensity of protein signals was quantified with Multigauge software, normalized to gel Coomassie blue staining, and expressed as a ratio to gain arbitrary densiometric units of relative abundance.

Antibodies against GLUT4, Akt, and P-Akt^{Ser473} for western blot were from Cell Signaling Technology (catalog nos. 2299, 4691, and 9271; Danvers, MA). Antibodies against AS160 and

P-AS160^{thr642} were from Millipore (07-741 and 07-802; Millipore, Billerica, MA) and horseradish peroxidase-conjugated anti-rabbit IgGs were from Sigma-Aldrich (A0545).

Immunofluorescence staining

The location of GLUT4 was determined by immunofluorescene staining of paraffin-embedded muscle sections with GLUT4 antibody (catalog no. ab33780, Abcam) as described (63). Slides were viewed on an Axiovert 200 confocal microscope (Zeiss, Jena, Germany) equipped with a laser-scanning confocal imaging LSM 510 META system (Carl Zeiss) and photomicrographed. Background settings were adjusted from examination of negative control specimens. Images of positive staining were adjusted to make optimal use of the dynamic range of detection. Control sections were stained with hematoxylin and eosin to illustrate nucleus of muscle cells.

Statistical analysis

Data are reported as mean ± SEM. Body weight gain at each time point was analyzed with a mixed between-within subjects ANOVA, followed by *t* test. Remaining analyses were tested with the Mann-Whitney U test where primary comparisons were between the PCOS and PCOS EA groups, and secondary comparisons were between controls and the PCOS groups. All statistical evaluations were performed with SPSS software (version 17.0, SPSS, Chicago, IL). $P < 0.05$ was considered significant.

RESULTS

After 4–5 weeks of low-frequency EA treatment, 11 of 12 rats (91.7%) in the PCOS EA group exhibited epithelial keratinocytes, the main cell type during estrus, indicating estrous cycle changes (23).

EA does not affect body composition

Rats with DHT-induced PCOS gained significantly more weight than controls, and they weighed more from 49 d of age (i.e., after 4 weeks of DHT exposure) and remained heavier throughout the study (Table 1). After 4 weeks of treatment (11 weeks of DHT exposure), the PCOS group had a higher percentage of fat mass along with a lower percentage of lean body mass, resulting in a higher ratio between body fat and lean body mass. They also had lower bone mineral content than controls (Table 2). Low-frequency EA did not affect body weight (Table 1) or body composition (Table 2).

The inguinal and parametrial adipose tissue depots were heavier in the PCOS group than in controls; the weights of retroperitoneal and mesenteric depots did not differ between the groups (Table 3). In relation to total body weight, the inguinal fat depot weighed more and the mesenteric depot weighed less in PCOS rats than in controls. Low-frequency EA increased retroperitoneal fat depots in both absolute and relative terms compared with PCOS rats with no treatment (Table 3).

The extensor digitorum longus, soleus, tibialis, and gastrocnemius muscles weighed more in the PCOS rats than in controls; however, in relation to total body weight, the soleus muscle weight was lower in PCOS rats (Table 3). Low-frequency EA in PCOS rats did not affect muscle weight.

EA restores normal insulin sensitivity in PCOS rats

All rats had similar basal insulin levels at the start of the euglycemic-hyperinsulinemic clamp. At steady state, plasma glucose levels were approximately ~6 mM, and the mean plasma insulin level was 284.45 ± 12.95 mU/L. The GIR was lower in PCOS rats than in controls,

indicating peripheral insulin resistance (Fig. 1). After 4–5 weeks of low-frequency EA, PCOS EA rats had significantly higher GIR than untreated PCOS rats (Fig. 1).

EA partly improves lipid profile in PCOS rats

Rats with DHT-induced PCOS had higher TG and LDL cholesterol levels than controls. After 4–5 weeks of low-frequency EA, however, the treated PCOS rats had lower total, HDL, and LDL cholesterol levels than untreated PCOS rats (Table 4).

EA increases GLUT4 protein expression in skeletal muscle of PCOS rats

To determine whether the beneficial effects of low-frequency EA on insulin sensitivity reflect alterations in protein expression in soleus muscle, we assessed GLUT4 and phosphorylated (P-) and nonphosphorylated Akt and AS160 by western blot. After 4–5 weeks of EA treatment, GLUT4 expression was significantly higher in the PCOS EA group than in untreated PCOS rats (Fig. 2A). The increased GLUT4 expression in the PCOS EA group was confirmed by immunofluorescence staining. In controls, GLUT4 was localized predominantly around the nucleus of muscle cells (Fig. 3A1-3 and E). In muscle cells from rats with DHT-induced PCOS, GLUT4 expression was less intense than in controls (Fig. 3B1-3), but GLUT4 expression in the plasma membrane and cytosol were increased by low-frequency EA (Fig. 3C1-3).

Continuous DHT exposure or intensive low-frequency EA did not affect the P-Akt/Akt (Fig. 2B) or the P-AS160/AS160 ratio (Fig. 2C) or expression of Akt, P-Akt, AS160, or P-AS160 (data not shown).

DISCUSSION

This study demonstrates that intensive low-frequency EA, given 5 d per week for 4–5 weeks, restores normal insulin sensitivity, as measured by euglycemic-hyperinsulinemic clamp, in rats

279 with DHT-induced PCOS. EA also increased expression of total GLUT4 in different
280 compartments of soleus muscle cells and partly improved the lipid profile in PCOS rats, which
281 may explain, at least in part, the improved insulin sensitivity. Since EA also improves ovarian
282 morphology and cyclicity (23, 51, 52), these findings suggest that EA interrupts the vicious cycle
283 of androgen excess, insulin resistance, and ovarian dysfunction in PCOS.

284 *How acupuncture may improve insulin sensitivity in DHT-induced PCOS*

285 Intramuscular needle insertion and stimulation cause a particular pattern of afferent activity
286 in peripheral nerve (Aδ and C) fibers (34) that leads to a variety of responses in the nervous
287 system as well as in the endocrine and metabolic systems. Low-frequency EA with repetitive
288 muscle contractions may activate physiological processes similar to those after physical exercise
289 (36), and EA increases responsiveness to insulin in normal rats and streptozotocin (STZ) diabetic
290 rats (8). The increases in insulin responsiveness in STZ diabetic rats and reduced hepatic glucose
291 output in normal rats after EA is at least partly mediated by mechanisms involving the activation
292 of sensory afferent and sympathetic efferent nerves (29, 65). Further, EA modulates the release
293 of endogenous opioids in the central nervous system and into the circulation, resulting in
294 activation of specific opioid receptors (26). In patients with diabetes, β-endorphin stimulates
295 insulin secretion by activating μ receptors in the pancreas (15). Recently, low-frequency EA in
296 abdominal acupoints lowered plasma glucose concentrations in rats with and without
297 hyperglycemia (9). This response was partly blocked by naloxone, a μ-opioid receptor
298 antagonist, suggesting that peripheral β-endorphin secretion participates in the regulation of
299 glucose concentrations (9, 43, 44). The hypoglycemic response to EA may also involve
300 serotonin, which also lower plasma glucose levels (10). Interestingly, naltrexone, another μ-

receptor antagonist, improves cyclicity, induces ovulation, and decreases LH, the LH/FSH ratio, and testosterone levels in women with PCOS (1, 24).

The physiological responses to acupuncture depend on many factors, including the number and placement of needles, the type of stimulation (manual, electrical with different frequencies), and the number and frequency of treatments. We placed the needles in abdominal and hind limb muscles and stimulated with a low frequency of 2 Hz with burst pulses of 0.1 s at 80 Hz to evoke muscle twitches. We used this stimulation modality, rather than needle penetration without electrical stimulation, because it has been systematically evaluated (68, 69). In our previous studies, low-frequency EA 3 d per week for 4–5 weeks improved insulin sensitivity and altered adipose tissue expression of genes related to obesity, insulin resistance, inflammation, and sympathetic activity without affecting adipose tissue mass or cellularity in DHT-induced PCOS rats (51, 52). However, the mechanism of these beneficial effects was unclear.

In this study, the frequency of treatment was increased to 5 d per week for 4–5 weeks. Remarkably, insulin sensitivity was restored to normal levels without affecting body weight/fat mass, most likely because of the increased number of treatments. Muscle contraction during low-frequency EA may stimulate glucose uptake via signaling pathway in skeletal muscle similar to those activated by chronic exercise (16, 25). Therefore, we tested the hypothesis that the beneficial effects on insulin sensitivity reflect alterations of protein expression in skeletal muscle. Soleus muscle was selected because it contains mostly slow-twitch oxidative muscle fibers (2), which are more responsive to insulin (67) and have greater insulin binding capacity (5). In addition, the percentage of oxidative muscle fibers correlates positively with glucose transport and GLUT4 content (28).

Improved skeletal muscle GLUT4 protein expression after low-frequency EA

Transport of glucose across the plasma cell membrane is the rate-limiting step in glucose metabolism and is primarily facilitated by five transmembrane proteins, GLUT1–5 (64). In rodent and human skeletal muscle, insulin stimulation or muscle contractions induce translocation of GLUT4 vesicles from intracellular depots to the plasma membrane, allowing for transport of glucose (47, 48, 57, 66). In women with PCOS, GLUT4 content in whole-cell lysates and membrane preparations is lower than in controls (60, 62). Consistent with these observations, GLUT4 expression in skeletal muscle in rats with DHT-induced PCOS tended to be decreased ($P = 0.091$). Low-frequency EA increased soleus GLUT4 expression which was confirmed by immunofluorescence staining. GLUT4 was localized predominantly around the nucleus of muscle cells in controls, and EA treatment increased GLUT4 expression in all compartments, including the plasma membrane of muscle cells. The apparent relative shift in the distribution of GLUT4 to the plasma membrane suggests a potential increase in transport capacity. Thus we speculate that the increased expression of GLUT4 may increase its translocation capability from other intracellular compartments to the plasma membrane, which may help explain the improved insulin sensitivity in PCOS rats. However, we cannot conclude from the immunofluorescence data alone that GLUT4 translocation increases after EA treatment.

This result indicates that low-frequency EA, given 5 times per week, activates signaling pathways similar to those activated by muscle contraction during exercise. It also indicates a ~~clear~~ dose-response relationship between the number of EA treatments and improvement in insulin sensitivity as compared with our previous trial (51, 52). Our results are in line with the acute effects of low-frequency EA in rats with prednisolone-induced insulin resistance, demonstrating increased skeletal muscle protein expression of insulin receptor substrate-1 and GLUT4 (45). Moreover, in the present study, the beneficial effects were at least semi-chronic,

since no treatment was performed 24 h before assessment of insulin sensitivity and tissue collection.

The euglycemic-hyperinsulinemic clamp with high insulin input may induce insulin-dependent signaling beyond the molecular events caused by low-frequency EA. However, insulin stimulation and muscle contraction have a combined effect that is larger than the net effect of either alone (46, 57). Thus contractions and insulin stimulation induce translocation of GLUT4 vesicles through diverse intracellular mechanisms.

In skeletal muscle and adipocytes, GLUT4 translocation induced by insulin or muscle contractions is at least partly dependent on phosphorylation of AS160 (38, 39, 61). However, the exact mechanism is unclear. Insulin-stimulated phosphorylation of AS160 is mediated by Akt, while contraction-stimulated phosphorylation is mediated by AMPK possibly together with Akt and other kinases (38). Although both Akt and AS160 seem to be involved in GLUT4 translocation, neither was affected by low-frequency EA. The reason for this may be that the experiment ended with euglycemic-hyperinsulinemic clamp with high insulin input, which may induce Akt phosphorylation, as in women with PCOS (11, 32), or the effect of EA may involve other insulin-independent signaling mechanisms. Further studies of Akt phosphorylation in skeletal muscle and adipose tissue, using lower insulin levels, are required to elucidate its role in DHT-induced PCOS.

Partly normalized lipid profile after low-frequency EA

Low-frequency EA for 4–5 weeks reduced total and LDL cholesterol in rats with DHT-induced PCOS. Interestingly, we found a decrease in HDL cholesterol. This result might seem conflicting with an otherwise improved lipid profile. However, mice and rats, compared to human, carry most of their serum cholesterol in the HDL fraction instead of the LDL

fraction.(27) Hence, it is not surprising that the demonstrated decrease in total cholesterol is reflective of changes in HDL cholesterol. EA also reduces total and LDL cholesterol in obese patients with hypercholesterolemia (7, 72) and in a rat model of hyperlipidemia (42). In comprehensive gene expression profile analyses, the cholesterol-lowering effect of EA in the liver of hypercholesterolemic mice was attributed to improved lipid metabolism and suppression of inflammation (35, 41). In line with these observations, we demonstrated that low-frequency EA decreases mRNA expression of inflammatory markers in mesenteric adipose tissue of rats with DHT-induced PCOS (52). In studies not related to PCOS, daily low-frequency EA treatment for 4 weeks in rats and humans reduced food intake and weight (6, 37). EA treatment has also been shown to improve lipid profile in mice (41) and humans (7). However, low-frequency EA administered 3 or 5 d per week in rats with DHT-induced PCOS does not affect body weight (52) and thus may not explain the improved lipid profile in the present experiment. Our studies have shown that EA improves ovarian morphology and restores altered adipose tissue gene expression related to insulin resistance, obesity, inflammation, and high sympathetic activity (51, 52). Thus, EA seems to disrupt the vicious circle of androgen excess, insulin resistance and ovarian dysfunction, despite continuous administration of androgens.

No change in body composition

As in our previous study (52), EA did not alter body composition measured by DEXA. Further, the weight of soleus was lower in relation to body weight in PCOS rats, however not affected by EA, despite the more frequent treatment (52). This implies that the normalization of insulin sensitivity in the present study is more likely due to molecular effects than to altered body composition or an increased glucose demand due to larger muscle mass. The discrepancy in muscle weight could simply reflect differences related to tissue dissection. Surprisingly, though,

EA increased the weight of the retroperitoneal fat depot, something not seen in the earlier study (52). The implications of this finding in relation to the increased insulin sensitivity are unclear.

Conclusion

Low-frequency EA given 5 d per week for 4–5 weeks restores normal insulin sensitivity, increases skeletal muscle protein expression of GLUT4 in different compartments of soleus muscle cells, and improves the lipid profile in rats with DHT-induced PCOS. Thus, low-frequency EA treatment has systemic and local effects involving intracellular signaling pathways in muscle that may account for the improved insulin sensitivity.

Acknowledgments

We thank Linda Backman for technical assistance. We also thank the Centre for Mouse Physiology and Bio-Imaging, University of Gothenburg. This study was financed by grants from the Swedish Medical Research Council (Project No. 2008-72VP-15445-01A), Novo Nordisk Foundation, Wilhelm and Martina Lundgrens's Science Fund, Hjalmar Svensson Foundation, Tore Nilson Foundation, Åke Wiberg Foundation, Adlerbert Research Foundation, Ekhaga Foundation, and the Swedish federal government under letters of understanding agreement of Medical Education (ALFFGBG-10984).

Conflict of interest

The authors confirm that there are no conflicts of interest.

REFERENCES

1. **Ahmed MI, Duleba AJ, El Shahat O, Ibrahim ME, and Salem A.** Naltrexone treatment in clomiphene resistant women with polycystic ovary syndrome. *Hum Reprod* 23: 2564-2569, 2008.
2. **Armstrong RB and Phelps RO.** Muscle fiber type composition of the rat hindlimb. *Am J Anat* 171: 259-272, 1984.
3. **Azziz R, Carmina E, Dewailly D, Diamanti-Kandarakis E, Escobar-Morreale HF, Futterweit W, Janssen OE, Legro RS, Norman RJ, Taylor AE, and Witchel SF.** The Androgen Excess and PCOS Society criteria for the polycystic ovary syndrome: the complete task force report. *Fertil Steril* 91: 456-488, 2009.
4. **Beloosesky R, Gold R, Almog B, Sasson R, Dantes A, Land-Bracha A, Hirsh L, Itskovitz-Eldor J, Lessing JB, Homburg R, and Amsterdam A.** Induction of polycystic ovary by testosterone in immature female rats: Modulation of apoptosis and attenuation of glucose/insulin ratio. *Int J Mol Med* 14: 207-215, 2004.
5. **Bonen A, Tan MH, and Watson-Wright WM.** Insulin binding and glucose uptake differences in rodent skeletal muscles. *Diabetes* 30: 702-704, 1981.
6. **Cabioglu MT and Ergene N.** Changes in serum leptin and beta endorphin levels with weight loss by electroacupuncture and diet restriction in obesity treatment. *Am J Chin Med* 34: 1-11, 2006.
7. **Cabioglu MT and Ergene N.** Electroacupuncture therapy for weight loss reduces serum total cholesterol, triglycerides, and LDL cholesterol levels in obese women. *Am J Chin Med* 33: 525-533, 2005.

8. **Chang S-L, Lin K-J, Lin R-T, Hung P-H, Lin J-G, and Cheng J-T.** Enhanced insulin sensitivity using electroacupuncture on bilateral Zusanli acupoints (ST 36) in rats. *Life Sciences* 79: 967-971, 2006.

9. **Chang SL, Lin JG, Chi TC, Liu IM, and Cheng JT.** An insulin-dependent hypoglycaemia induced by electroacupuncture at the Zhongwan (CV12) acupoint in diabetic rats. *Diabetologia* 42: 250-255, 1999.

10. **Chang SL, Tsai CC, Lin JG, Hsieh CL, Lin RT, and Cheng JT.** Involvement of serotonin in the hypoglycemic response to 2 Hz electroacupuncture of zusanli acupoint (ST36) in rats. *Neurosci Lett* 379: 69-73, 2005.

11. **Ciaraldi TP, Aroda V, Mudaliar S, Chang RJ, and Henry RR.** Polycystic Ovary Syndrome Is Associated with Tissue-Specific Differences in Insulin Resistance. *J Clin Endocrinol Metab* 94: 157-163, 2009.

12. **Ciaraldi TP, el-Roeiy A, Madar Z, Reichart D, Olefsky JM, and Yen SS.** Cellular mechanisms of insulin resistance in polycystic ovarian syndrome. *J Clin Endocrinol Metab* 75: 577-583, 1992.

13. **Corbould A.** Effects of androgens on insulin action in women: is androgen excess a component of female metabolic syndrome? *Diabetes/metabolism research and reviews* 24: 520-532, 2008.

14. **Coviello AD, Legro RS, and Dunaif A.** Adolescent girls with polycystic ovary syndrome have an increased risk of the metabolic syndrome associated with increasing androgen levels independent of obesity and insulin resistance. *J Clin Endocrinol Metab* 91: 492-497, 2006.

15. **Curry DL, Bennett LL, and Li CH.** Stimulation of insulin secretion by beta-endorphins (1-27 & 1-31). *Life Sci* 40: 2053-2058, 1987.

16. **Deshmukh AS, Hawley JA, and Zierath JR.** Exercise-induced phospho-proteins in skeletal muscle. *Int J Obes (Lond)* 32 Suppl 4: S18-23, 2008.

17. **Diamond MP, Grainger D, Diamond MC, Sherwin RS, and Defronzo RA.** Effects of methyltestosterone on insulin secretion and sensitivity in women. *J Clin Endocrinol Metab* 83: 4420-4425, 1998.

18. **Dunaif A.** Insulin resistance and the polycystic ovary syndrome: mechanism and implications for pathogenesis. *Endocr Rev* 18: 774-800., 1997.

19. **Dunaif A and Finegood DT.** Beta-cell dysfunction independent of obesity and glucose intolerance in the polycystic ovary syndrome. *J Clin Endocrinol Metab* 81: 942-947, 1996.

20. **Dunaif A, Segal KR, Shelley DR, Green G, Dobrjansky A, and Licholai T.** Evidence for distinctive and intrinsic defects in insulin action in polycystic ovary syndrome. *Diabetes* 41: 1257-1266, 1992.

21. **Dunaif A, Wu X, Lee A, and Diamanti-Kandarakis E.** Defects in insulin receptor signaling in vivo in the polycystic ovary syndrome (PCOS). *Am J Physiol Endocrinol Metab* 281: E392-399, 2001.

22. **Elbers JM, Asscheman H, Seidell JC, Megens JA, and Gooren LJ.** Long-term testosterone administration increases visceral fat in female to male transsexuals. *J Clin Endocrinol Metab* 82: 2044-2047, 1997.

23. **Feng Y, Johansson J, Shao R, Manneras L, Fernandez-Rodriguez J, Billig H, and Stener-Victorin E.** Hypothalamic neuroendocrine functions in rats with dihydrotestosterone-induced polycystic ovary syndrome: effects of low-frequency electro-acupuncture. *PLoS One* 4: e6638, 2009.

24. **Fruzzetti F, Bersi C, Parrini D, Ricci C, and Genazzani AR.** Effect of long-term naltrexone treatment on endocrine profile, clinical features, and insulin sensitivity in obese women with polycystic ovary syndrome. *Fertil Steril* 77: 936-944, 2002.

25. **Goodyear LJ and Kahn BB.** Exercise, glucose transport, and insulin sensitivity. *Annu Rev Med* 49: 235-261, 1998.

26. **Han J-S.** Acupuncture: neuropeptide release produced by electrical stimulation of different frequencies. *Trends in Neurosciences* 26: 17-22, 2003.

27. **Harris WS.** n-3 fatty acids and serum lipoproteins: animal studies. *Am J Clin Nutr* 65: 1611S-1616S, 1997.

28. **Henriksen EJ, Bourey RE, Rodnick KJ, Koranyi L, Permutt MA, and Holloszy JO.** Glucose transporter protein content and glucose transport capacity in rat skeletal muscles. *Am J Physiol* 259: E593-598, 1990.

29. **Higashimura Y, Shimoju R, Maruyama H, and Kurosawa M.** Electro-acupuncture improves responsiveness to insulin via excitation of somatic afferent fibers in diabetic rats. *Auton Neurosci* 150: 100-103, 2009.

30. **Holmang A, Niklasson M, Rippe B, and Lonnroth P.** Insulin insensitivity and delayed transcapillary delivery of insulin in oophorectomized rats treated with testosterone. *Acta Physiol Scand* 171: 427-438, 2001.

31. **Holmang A, Svedberg J, Jennische E, and Bjorntorp P.** Effects of testosterone on muscle insulin sensitivity and morphology in female rats. *Am J Physiol* 259: E555-560, 1990.

32. **Højlund K, Glintborg D, Andersen NR, Birk JB, Treebak JT, FrÃ¸sig C, Beck-Nielsen H, and Wojtaszewski JrFP.** Impaired Insulin-Stimulated Phosphorylation of Akt and

AS160 in Skeletal Muscle of Women With Polycystic Ovary Syndrome Is Reversed by Pioglitazone Treatment. *Diabetes* 57: 357-366, 2008.

33. **Ishizaki N, Okushi N, Yano T, and Yamamura Y.** Improvement in glucose tolerance as a result of enhanced insulin sensitivity during electroacupuncture in spontaneously diabetic Goto-Kakizaki rats. *Metabolism* 58: 1372-1378, 2009.
34. **Kagitani F, Uchida S, Hotta H, and Aikawa Y.** Manual acupuncture needle stimulation of the rat hindlimb activates groups I, II, III and IV single afferent nerve fibers in the dorsal spinal roots. *Jpn J Physiol* 55: 149-155, 2005.
35. **Kang Y, Li M, Yan W, Li X, Kang J, and Zhang Y.** Electroacupuncture alters the expression of genes associated with lipid metabolism and immune reaction in liver of hypercholesterolemia mice. *Biotechnol Lett* 29: 1817-1824, 2007.
36. **Kaufman MP, Waldrop TG, Rybycki KJ, Ordway GA, and Mitchell JH.** Effects of static and rythmic twitch contractions on the discharge of group III and IV muscle afferents. *Cardiovasc Rec* 18: 663-668, 1984.
37. **Kim SK, Lee G, Shin M, Han JB, Moon HJ, Park JH, Kim KJ, Ha J, Park DS, and Min BI.** The association of serum leptin with the reduction of food intake and body weight during electroacupuncture in rats. *Pharmacol Biochem Behav* 83: 145-149, 2006.
38. **Kramer HF, Witczak CA, Fujii N, Jessen N, Taylor EB, Arnolds DE, Sakamoto K, Hirshman MF, and Goodyear LJ.** Distinct signals regulate AS160 phosphorylation in response to insulin, AICAR, and contraction in mouse skeletal muscle. *Diabetes* 55: 2067-2076, 2006.
39. **Larance M, Ramm G, Stöckli J, van Dam EM, Winata S, Wasinger V, Simpson F, Graham M, Junutula JR, Guilhaus M, and James DE.** Characterization of the role of the

Rab GTPase-activating protein AS160 in insulin-regulated GLUT4 trafficking. *J Biol Chem* 280: 37803-37813, 2005.

40. **Legro RS.** Polycystic ovary syndrome. Phenotype to genotype. *Endocrinol Metab Clin North Am* 28: 379-396, 1999.

41. **Li M and Zhang Y.** Modulation of gene expression in cholesterol-lowering effect of electroacupuncture at Fenglong acupoint (ST40): a cDNA microarray study. *Int J Mol Med* 19: 617-629, 2007.

42. **Li X, Zhu J, and Huo H.** Profile of differentially expressed genes in blood vessels and blood cells of hyperlipidemia rats using suppression subtractive hybridization. *J Nanosci Nanotechnol* 5: 1287-1291, 2005.

43. **Lin J-G, Chen W-C, Hsieh C-L, Tsai C-C, Cheng Y-w, Cheng J-T, and Chang S-L.** Multiple sources of endogenous opioid peptide involved in the hypoglycemic response to 15 Hz electroacupuncture at the Zhongwan acupoint in rats. *Neurosci Lett* 366: 39-42, 2004.

44. **Lin JG, Chang SL, and Cheng JT.** Release of beta-endorphin from adrenal gland to lower plasma glucose by the electroacupuncture at Zhongwan acupoint in rats. *Neurosci Lett* 326: 17-20, 2002.

45. **Lin RT, Tzeng CY, Lee YC, Ho WJ, Cheng JT, Lin JG, and Chang SL.** Acute effect of electroacupuncture at the Zusanli acupoints on decreasing insulin resistance as shown by lowering plasma free fatty acid levels in steroid-background male rats. *BMC Complement Altern Med* 9: 26, 2009.

46. **Lund S, Holman GD, Schmitz O, and Pedersen O.** Contraction stimulates translocation of glucose transporter GLUT4 in skeletal muscle through a mechanism distinct from that of insulin. *Proc Natl Acad Sci U S A* 92: 5817-5821, 1995.

47. **Lund S, Holman GD, Schmitz O, and Pedersen O.** Glut 4 content in the plasma membrane of rat skeletal muscle: comparative studies of the subcellular fractionation method and the exofacial photolabelling technique using ATB-BMPA. *FEBS Letters* 330: 312-318, 1993.

48. **Lund S, Holman GD, Zierath JR, Rincon J, Nolte LA, Clark AE, Schmitz O, Pedersen O, and Wallberg-Henriksson H.** Effect of insulin on GLUT4 cell surface content and turnover rate in human skeletal muscle as measured by the exofacial bis-mannose photolabeling technique. *Diabetes* 46: 1965-1969, 1997.

49. **Macut D, Panidis D, Glisic B, Spanos N, Petakov M, Bjekic J, Stanojlovic O, Rousso D, Kourtis A, Bozic I, and Damjanovic S.** Lipid and lipoprotein profile in women with polycystic ovary syndrome. *Can J Physiol Pharmacol* 86: 199-204, 2008.

50. **Manneras L, Cajander S, Holmang A, Seleskovic Z, Lystig T, Lonn M, and Stener-Victorin E.** A new rat model exhibiting both ovarian and metabolic characteristics of Polycystic Ovary Syndrome. *Endocrinology* 148: 3781-3791, 2007.

51. **Manneras L, Cajander S, Lonn M, and Stener-Victorin E.** Acupuncture and exercise restore adipose tissue expression of sympathetic markers and improve ovarian morphology in rats with dihydrotestosterone-induced PCOS. *Am J Physiol Regul Integr Comp Physiol* 296: R1124-1131, 2009.

52. **Manneras L, Jonsdottir IH, Holmang A, Lonn M, and Stener-Victorin E.** Low-Frequency Electro-Acupuncture and Physical Exercise Improve Metabolic Disturbances and Modulate Gene Expression in Adipose Tissue in Rats with Dihydrotestosterone-Induced Polycystic Ovary Syndrome. *Endocrinology* 149: 3559-3568, 2008.

53. **Manni L, Lundeberg T, Holmang A, Aloe L, and Stener-Victorin E.** Effect of electro-acupuncture on ovarian expression of alpha (1)- and beta (2)-adrenoceptors, and p75 neurotrophin receptors in rats with steroid-induced polycystic ovaries. *Reprod Biol Endocrinol* 3: 21, 2005.

54. **Marcondes FK, Bianchi FJ, and Tanno AP.** Determination of the estrous cycle phases of rats: some helpful considerations. *Braz J Biol* 62: 609-614, 2002.

55. **Moran LJ, Pasquali R, Teede HJ, Hoeger KM, and Norman RJ.** Treatment of obesity in polycystic ovary syndrome: a position statement of the Androgen Excess and Polycystic Ovary Syndrome Society. *Fertil Steril* 92: 1966-1982, 2008.

56. **Norman RJ, Dewailly D, Legro RS, and Hickey TE.** Polycystic ovary syndrome. *Lancet* 370: 685-697, 2007.

57. **Ploug T, van Deurs B, Ai H, Cushman SW, and Ralston E.** Analysis of GLUT4 Distribution in Whole Skeletal Muscle Fibers: Identification of Distinct Storage Compartments That Are Recruited by Insulin and Muscle Contractions. *J Cell Biol* 142: 1429-1446, 1998.

58. **Rincon J, Holmang A, Wahlstrom EO, Lonnroth P, Bjorntorp P, Zierath JR, and Wallberg-Henriksson H.** Mechanisms behind insulin resistance in rat skeletal muscle after oophorectomy and additional testosterone treatment. *Diabetes* 45: 615-621, 1996.

59. **Rockl KS, Witczak CA, and Goodyear LJ.** Signaling mechanisms in skeletal muscle: acute responses and chronic adaptations to exercise. *IUBMB Life* 60: 145-153, 2008.

60. **Rosenbaum D, Haber RS, and Dunaif A.** Insulin resistance in polycystic ovary syndrome: decreased expression of GLUT-4 glucose transporters in adipocytes. *Am J Physiol Endocrinol Metab* 264: E197-202, 1993.

61. **Sano H, Kane S, Sano E, Mîinea CP, Asara JM, Lane WS, Garner CW, and Lienhard GE.** Insulin-stimulated phosphorylation of a Rab GTPase-activating protein regulates GLUT4 translocation. *J Biol Chem* 278: 14599-14602, 2003.

62. **Seow K-M, Juan C-C, Hsu Y-P, Hwang J-L, Huang L-W, and Ho L-T.** Amelioration of insulin resistance in women with PCOS via reduced insulin receptor substrate-1 Ser312 phosphorylation following laparoscopic ovarian electrocautery. *Hum Reprod* 22: 1003-1010, 2007.

63. **Shao R, Weijdegard B, Fernandez-Rodriguez J, Egecioglu E, Zhu C, Andersson N, Thurin-Kjellberg A, Bergh C, and Billig H.** Ciliated epithelial-specific and regional-specific expression and regulation of the estrogen receptor-beta2 in the fallopian tubes of immature rats: a possible mechanism for estrogen-mediated transport process in vivo. *Am J Physiol Endocrinol Metab* 293: E147-158, 2007.

64. **Shepherd PR and Kahn BB.** Glucose Transporters and Insulin Action -- Implications for Insulin Resistance and Diabetes Mellitus. *N Engl J Med* 341: 248-257, 1999.

65. **Shimoju-Kobayashi R, Maruyama H, Yoneda M, and Kurosawa M.** Responses of hepatic glucose output to electro-acupuncture stimulation of the hindlimb in anaesthetized rats. *Auton Neurosci* 115: 7-14, 2004.

66. **Slot J, Geuze H, Gigengack S, Lienhard G, and James D.** Immuno-localization of the insulin regulatable glucose transporter in brown adipose tissue of the rat. *J Cell Biol* 113: 123-135, 1991.

67. **Song XM, Ryder JW, Kawano Y, Chibalin AV, Krook A, and Zierath JR.** Muscle fiber type specificity in insulin signal transduction. *Am J Physiol Regul Integr Comp Physiol* 277: R1690-1696, 1999.

68. **Stener-Victorin E, Fujisawa S, and Kurosawa M.** Ovarian blood flow responses to electroacupuncture stimulation depend on estrous cycle and on site and frequency of stimulation in anesthetized rats. *J Appl Physiol* 101: 84-91, 2006.

69. **Stener-Victorin E, Kobayashi R, and Kurosawa M.** Ovarian blood flow responses to electro-acupuncture stimulation at different frequencies and intensities in anaesthetized rats. *Auton Neurosci* 108: 50-56, 2003.

70. **Stener-Victorin E, Kobayashi R, Watanabe O, Lundeberg T, and Kurosawa M.** Effect of electro-acupuncture stimulation of different frequencies and intensities on ovarian blood flow in anaesthetized rats with steroid-induced polycystic ovaries. *Reprod Biol Endocrinol* 2: 16, 2004.

71. **Stener-Victorin E, Lundeberg T, Cajander S, Aloe L, Manni L, Waldenstrom U, and Janson PO.** Steroid-induced polycystic ovaries in rats: effect of electro-acupuncture on concentrations of endothelin-1 and nerve growth factor (NGF), and expression of NGF mRNA in the ovaries, the adrenal glands, and the central nervous system. *Reprod Biol Endocrinol* 1: 33, 2003.

72. **Wang YT and An H.** The acupuncture at Fenglong acupoint for treatment of 49 cases of hypercholestrolemia. *Chin Acupunct Moxibust* 3: 21-23, 1990.

635 **TABLE 1.** Weight development during the study

Age (d)	Body weight (g)				
	Control (n = 12)	PCOS (n = 12)	PCOS EA (n = 12)	PCOS vs. Control	PCOS vs. PCOS EA
21	49 ± 1	49 ± 2	48 ± 2	ns	ns
28	80 ± 2	83 ± 4	80 ± 3	ns	ns
35	131 ± 3	130 ± 4	131 ± 4	ns	ns
42	157 ± 3	168 ± 4	176 ± 4	ns	ns
49	186 ± 3	207 ± 5	214 ± 4	$P < 0.001$	ns
56	209 ± 4	244 ± 6	249 ± 5	$P < 0.001$	ns
63	228 ± 3	272 ± 5	282 ± 5	$P < 0.001$	ns
70	241 ± 3	287 ± 5	299 ± 6	$P < 0.001$	ns
77	251 ± 4	297 ± 6	309 ± 6	$P < 0.001$	ns
84	256 ± 4	307 ± 6	319 ± 7	$P < 0.001$	ns
91	257 ± 5	310 ± 7	324 ± 7	$P < 0.001$	ns
End of exp.	262 ± 5	321 ± 7	333 ± 7	$P < 0.001$	ns

636 Values are mean ± SEM. ns, not significant. Mixed between-within subjects ANOVA was significant (P
637 < 0.05). Differences between groups at each time point were determined by t test.
638

639 **TABLE 2**. Effects of low frequency electro-acupuncture (EA) on body composition estimated by DEXA

Variable	Control (n = 12)	PCOS (n = 12)	PCOS EA (n = 12)	PCOS vs. Control	PCOS vs. PCOS EA
Body fat (% of BW)	15.4 ± 0.9	19.5 ± 1.0	19.5 ± 1.6	$P < 0.01$	ns
Body fat (g)	39.1 ± 3.1	59.6 ± 3.4	51.8 ± 5.9	$P < 0.001$	ns
LBM (% of BW)	81.9 ± 0.8	78.0 ± 1.0	78.0 ± 1.6	$P < 0.01$	ns
LBM (g)	206.1 ± 3.6	237.8 ± 6.0	245.2 ± 6.9	$P < 0.001$	ns
BMC (% of BW)	2.8 ± 0	2.5 ± 0	2.5 ± 0	$P < 0.001$	ns
BMC (g)	6.9 ± 0.1	7.7 ± 0.2	8.1 ± 0.2	$P < 0.01$	ns
Body fat (g)/LBM (g)	0.19 ± 0.01	0.25 ± 0.02	0.27 ± 0.03	$P < 0.01$	ns

640 Values are mean ± SEM. BW, body weight; LBM, lean body mass; BMC, bone mineral content; ns, not
641 significant. Statistical significance was determined with the Mann-Whitney U-test
642

643 **TABLE 3.** Weight of dissected individual fat depots and muscles in DHT-induced PCOS compared with
644 controls and the effect of low frequency electro-acupuncture (EA) treatment

Variable	Control (n = 11)	PCOS (n = 11)	PCOS EA (n = 12)	PCOS vs. Control	PCOS vs. PCOS EA
Fat depots (g)					
Inguinal	1.18 ± 0.07	2.23 ± 0.13	2.22 ± 0.17	$P < 0.001$	ns
Parametrial	3.75 ± 0.38	6.93 ± 0.37	5.08 ± 0.77	$P < 0.05$	ns
Retroperitoneal	2.17 ± 0.11	2.31 ± 0.09	2.48 ± 0.11	ns	$P < 0.05$
Mesenteric	2.68 ± 0.19	2.94 ± 0.19	2.61 ± 0.18	ns	ns
Fat depots (g/kg BW)					
Inguinal	4.47 ± 0.21	6.93 ± 0.37 [C]	6.63 ± 0.42	$P < 0.001$	ns
Parametrial	14.20 ± 1.21	16.22 ± 1.23	15.17 ± 2.15	ns	ns
Retroperitoneal	8.83 ± 0.64	8.14 ± 0.54	10.81 ± 0.81	ns	$P < 0.05$
Mesenteric	8.26 ± 0.29	7.10 ± 0.28	7.43 ± 0.32	$P < 0.01$	ns
Muscles (g)					
EDL	0.12 ± 0.004	0.28 ± 0.01	0.28 ± 0.01	$P < 0.001$	ns
Soleus	0.13±0.003	0.14 ± 0.05	0.14 ± 0.003	$P < 0.05$	ns
Tibialis	0.54 ± 0.01	0.63 ± 0.01	0.64 ± 0.02	$P < 0.001$	ns
Gastrocnemius	4.92 ± 0.15	5.22 ± 0.12	4.91 ± 0.17	$P < 0.001$	ns
Muscles (g/kg BW)					
EDL	0.47 ± 0.02	0.47 ± 0.01	0.47 ± 0.016	ns	ns
Soleus	0.50 ± 0.01	0.44 ± 0.01	0.44 ± 0.01	$P < 0.01$	ns
Tibialis	2.05±0.04	1.99 ± 0.04	1.92 ± 0.05	ns	ns
Gastrocnemius	4.92 ± 0.15	5.21 ± 0.12	4.91 ± 0.17	ns	ns

645 Values are mean ± SEM. BW, body weight; EDL, extensor digitorum longus; ns, not significant.
646 Statistical significance was determined with the Mann-Whitney U-test.
647

TABLE 4. Fasting serum concentrations of total cholesterol, triglycerides, HDL and LDL in DHT induced PCOS compared to controls and effect of intensive low-frequency electro-acupuncture (EA) treatment

Variable	Control (n = 12)	PCOS (n = 12)	PCOS EA (n = 12)	PCOS vs. Control	PCOS vs. PCOS EA
Cholesterol	2.49 ± 0.11	2.37 ± 0.11	2.11 ± 0.07	ns	$P < 0.05$
Triglycerides	0.82 ± 0.08	1.19 ± 0.08	1.05 ± 0.06	$P < 0.01$	ns
HDL	2.05 ± 0.10	1.96 ± 0.10	1.71 ± 0.08	ns	$P < 0.05$
LDL	0.36 ± 0.03	0.43 ± 0.03	0.36 ± 0.02	$P < 0.01$	$P < 0.05$

Values are mean ± SEM. ns, not significant. Statistical significance was determined with the Mann-Whitney U-test.

654 **FIGURE LEGENDS**

655 **Figure 1.** GIR in controls (n=11), rats with DHT-induced PCOS (n=11), and PCOS EA rats
656 (n=12) after 4–5 weeks of treatment/handling. Values are mean ± SEM. ***$P < 0.001$ vs.
657 control, $^{###}P < 0.001$ vs. PCOS (Mann-Whitney U test).

658 **Figure 2:** (A) Protein content of GLUT4 (control n=8, PCOS n=10, PCOS EA n=11), (B) P-
659 Akt/Akt ratio (control n=9, PCOS n=10, PCOS EA n=11), and (C) P-AS160/AS160 ratio
660 (control n=9, PCOS n = 11, PCOS EA n=12) in rat soleus muscles detected by western blot after
661 4–5 weeks of treatment/handling. Top: Lysates (30–50 μg) were separated by SDS-PAGE.
662 Representative immunoblots from independent samples are shown. Bottom: Densiometric
663 analysis of protein expression. Equal loading was confirmed by Coomassie Blue staining, and
664 protein levels were expressed as a ratio to the densiometric value of whole proteins in Coomassie
665 Blue–stained gels. Values are means ± SEM. $^{#}P < 0.05$ vs. PCOS (Mann-Whitney U test).
666

667 **Figure 3:** Expression of GLUT4 in muscle cells in controls, rats with DHT-induced PCOS, and
668 PCOS EA rats. Although the immunoreactivity of GLUT4 is less intense in DHT-induced PCOS
669 rat muscle cells (B1-3) than in controls, GLUT4 is predominantly localized around the nucleus
670 of the muscle cells (A1-3). EA treatment (C1-3) increases GLUT4 expression in the plasma
671 membrane and in the cytosol of muscle cells. Muscle GLUT4 immunoreactivity was absent in
672 the adjacent section when the primary antibody was omitted (D). Staining was repeated in four
673 rats/group with similar results. The immunofluorescence findings shown are representative of
674 those in randomly selected sections from multiple animals. Hematoxylin-eosin staining in control
675 rats illustrate nucleus of muscle cells (E). All photographs were taken with a 20x objective; the
676 exact scale is given in the figure.

Figure 1

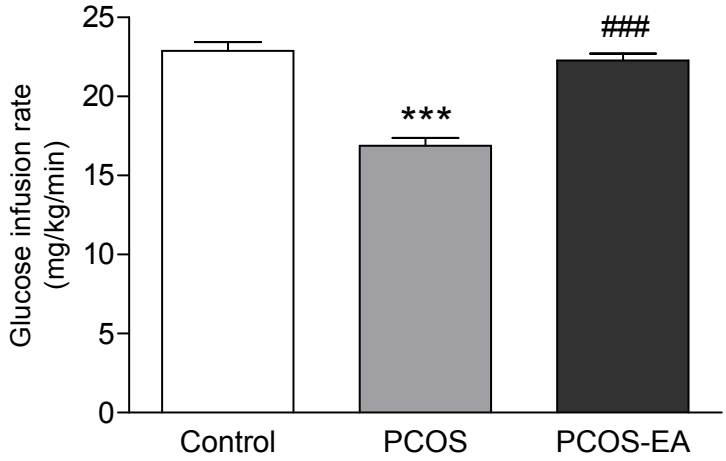
Glucose infusion rate
(mg/kg/min)
25
20
15
10
5
0
***
###
Control
PCOS
PCOS-EA

Figure 2

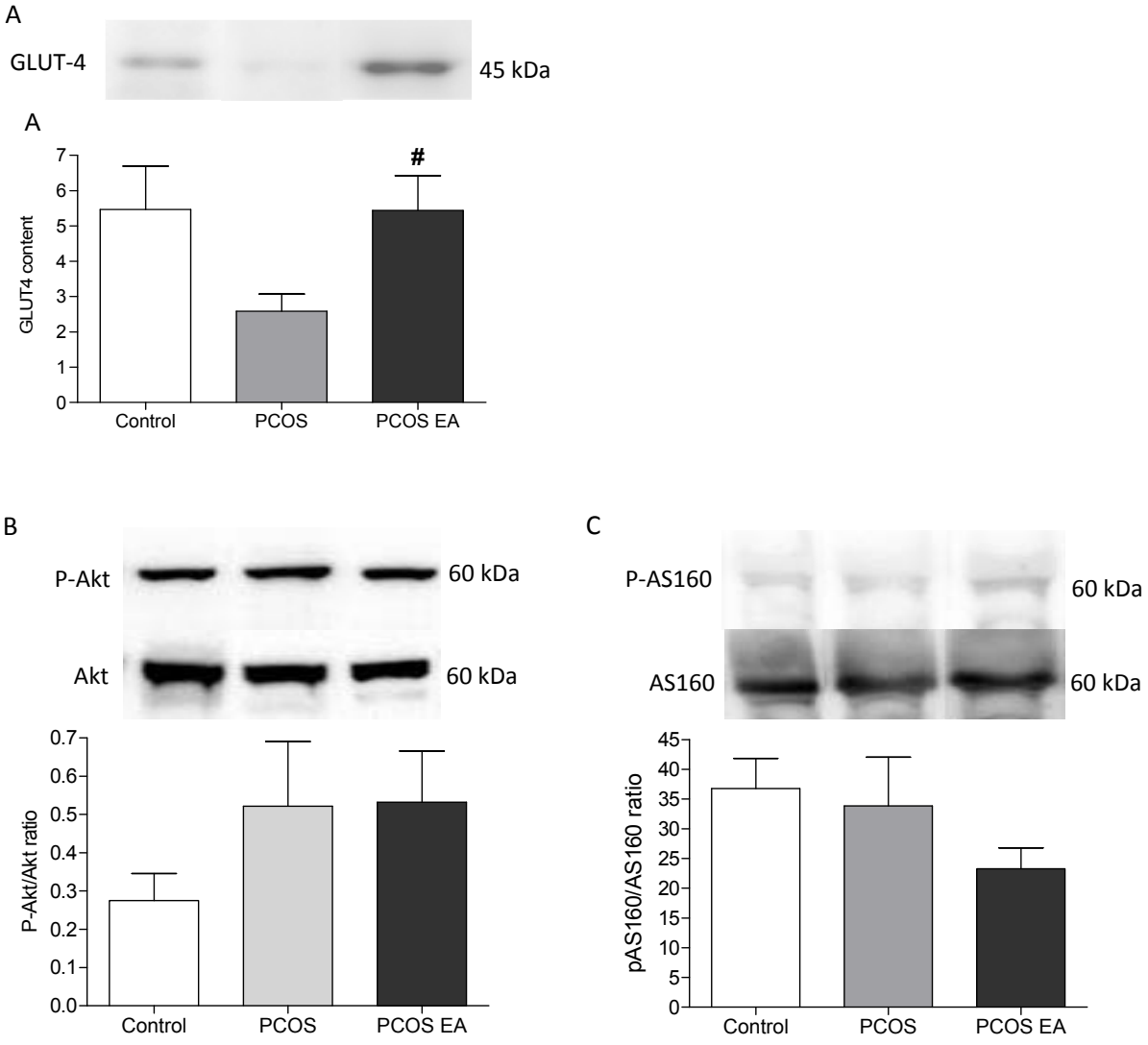
A
GLUT-4
45 kDa
A
GLUT4 content
#
Control
PCOS
PCOS EA
B
P-Akt
60 kDa
Akt
60 kDa
P-Akt/Akt ratio
Control
PCOS
PCOS EA
C
P-AS160
60 kDa
AS160
60 kDa
pAS160/AS160 ratio
Control
PCOS
PCOS EA

Figure 3